agronomy

MDPI

Article

Low-Phytate Grains to Enhance Phosphorus Sustainability in Agriculture: Chasing Drought Stress in *lpa1-1* Mutant

Federico Colombo [1], Greta Bertagnon [1], Martina Ghidoli [1], Michele Pesenti [1], Luca Giupponi [2] and Roberto Pilu [1,*]

[1] Department of Agricultural and Environmental Sciences—Production, Landscape, Agroenergy, University of Milan, Via G. Celoria 2, 20133 Milan, Italy; federico.colombo@unimi.it (F.C.); greta.bertagnon@studenti.unimi.it (G.B.); martina.ghidoli@unimi.it (M.G.); michele.pesenti@unimi.it (M.P.)
[2] Centre of Applied Studies for the Sustainable Management and Protection of Mountain Areas—CRC Ge.S.Di.Mont., University of Milan, Via Morino 8, 25048 Edolo, Italy; luca.giupponi@unimi.it
* Correspondence: salvatore.pilu@unimi.it

Abstract: Phytic acid (PA) is an anti-nutritional factor for monogastrics and contributes to phosphorus pollution. The *low phytic acid* (*lpa)* trait can provide several benefits to the nutritional quality of foods/feeds and to environmental sustainability. In maize, four *lpa1* mutants have been isolated, and *lpa1-1* is the most promising. Nevertheless, these mutations are frequently accompanied by many negative pleiotropic effects affecting plant performance. One of these is a greater susceptibility to drought stress, probably caused by an alteration in the root system. In this work, we set up an experiment in hydroponics and two in mesocosms, where pots were built using transparent PVC sheets to better access the roots. The results suggested that neither root architecture nor root depth are limiting factors in mutant plants. In hydroponics, the dry weight of the mutant and the root area per unit of length were twice that of B73. However, *lpa1-1* exhibited a reduced efficiency of photosystem II (Fv/Fm, 0.810 vs. 0.800) and a reduced leaf temperature (−0.5 °C compared to wild-type), probably due to increased water loss. Furthermore, molecular analysis performed on genes involved in root development (*rtcs*, *rtcl*, *rum1*, and *BIGE1)* revealed the abundance of *rtcs* transcripts in the mutant, suggesting an alteration in auxin polar transport.

Keywords: phosphorus; low phytic acid mutants; phytic acid; drought stress; root system architecture; environmental sustainability; agrobiodiversity

Citation: Colombo, F.; Bertagnon, G.; Ghidoli, M.; Pesenti, M.; Giupponi, L.; Pilu, R. Low-Phytate Grains to Enhance Phosphorus Sustainability in Agriculture: Chasing Drought Stress in *lpa1-1* Mutant. *Agronomy* **2022**, *12*, 721. https://doi.org/10.3390/agronomy12030721

Academic Editor: Mick Fuller

Received: 3 February 2022
Accepted: 11 March 2022
Published: 16 March 2022

1. Introduction

Phytic acid (PA) (myo-inositol-1,2,3,4,5,6-hexakisphosphate) is the most common storage form of phosphorus (P) in plant seeds [1]. In maize, PA is mainly located in the scutellum and only small quantities are present in the aleurone layer [2]. Phytic acid is accumulated in the protein storage vacuole as phytate mixed salts with different cations (particularly iron and zinc), reducing their bioavailability [3]. During germination, these salts are degraded by the activity of the phytase enzyme, releasing free phosphorus, myo-inositol, and minerals, essential for seedling growth [4]. Only ruminants are able to degrade phytic acid due to the presence of phytases in their digestive system. However, monogastric animals do not possess this enzyme: only the 10% of phytate in the feed is assimilated, while the remainder is excreted, contributing to P pollution and water surface eutrophication. Therefore, farmers must supply mineral phosphorus to the feed of monogastric animals, thus implying an economic problem [5]. Despite being considered an anti-nutritional factor for all these reasons, phytic acid plays a key role as an antioxidant compound. In fact, by chelating iron cations, PA can counteract the formation of reactive oxygen species (ROS), thus preserving the viability of seeds [6,7].

Some breeding programs have analyzed the genetic variability of both phytic acid and inorganic phosphorus present in a set of fifty inbred lines representing the Iowa lines from

B73 to B129 [8,9]. In particular Lorenz and colleagues reported phytic acid values ranging between 2.40–4.09 mg/g for fifty different maize lines [8]. However, the most promising strategy concerns the use of *low phytic acid* (*lpa*) mutants in which the PA content drops to around 1 mg/g [10].

In recent decades, many *lpa* mutants have been isolated in several crops: maize [10–13], wheat [14], barley [15–17], rice [18,19], soybean [20–22], and common bean [23,24]. The *lpa* trait can provide important benefits to the nutritional quality of foods and feeds and can contribute to the environmental sustainability of phosphorus in agriculture.

In maize, three different *low phytic acid* mutants have been isolated and characterized: *lpa1* [10,11], *lpa2* [10], and *lpa3* [25]. Among these, *lpa1* showed the greatest reduction of PA in the seed, followed by a proportional increase of free *P* without altering the total *P* content. Transposon mutagenesis experiments demonstrated that the gene *ZmMRP4* (accession number EF86878) is responsible for the *lpa1* mutation [26]. *ZmMRP4* is a multidrug resistance-associated protein (MRP) that belongs to the subfamily of ATP-binding cassette (ABC) transmembrane transporters [26]. The majority of *lpa* mutants carry mutations in genes that code for MRP proteins, and thus result in a lack of PA transfer from the cytosol to the vacuole. In maize, four *lpa1* mutants have been isolated so far: *lpa1-1* [26], *lpa1-241* [27,28], *lpa1-7* [12], and *lpa1-5525* (not fully characterized) [13]. *Lpa1-241* and *lpa1-7* are not viable in the homozygous state, displaying an 80–90% decrease in PA [12,27], while *lpa1-1* is the most promising *lpa1* mutant, showing a 66% reduction in phytic acid, followed by a proportional increase in inorganic phosphorus [10]. Unfortunately, the reduction of PA in *lpa1* mutations leads to various negative pleiotropic effects on the seed and, in general, on plant performance, as recently reviewed by Colombo et al. [29]. One of these agronomic defects observed in the field on the mutant *lpa1-1* is an increased susceptibility to drought stress, which might be caused by an alteration in the root system architecture (RSA) [12].

In maize, the root system includes embryonic and post-embryonic roots [30,31]: the former are important for seedling vigor in the early stages of development [32] and include the primary root and a variable number of seminal roots [33], while the post-embryonic root system dominates the RSA of adult plants [34]: it is formed by shoot-borne roots and includes crown roots (at underground nodes of the shoot) and brace roots (at aboveground nodes) [31]. All these types of roots generate postembryonic lateral roots, increasing the absorbing surface of the maize root system [35]. In recent decades, several genes that control maize root development have been isolated and characterized [36–39]. Genetic analyses conducted on maize revealed that many genes (*rtcs*, *rtcl*, *rum1*, and *BIGE1*) involved in auxin signal transduction are fundamental elements for the development of lateral, seminal, and shoot-borne roots [40]. The *rtcs* (rootless concerning crown and seminal roots) mutant was identified for the first time by Hetz et al. [41] by the complete lack of embryonically seminal roots and post-embryonically shoot-borne roots. The gene *rtcl* (rtcs-like) is the paralog of *rtcs* [36]: the coordinated function of these two paralogous genes in maize root initiation and elongation was reported in Xu et al., 2015 [39]. The *rum1* (rootless with undetectable meristems 1) mutant is defective in seminal roots and lateral roots at the primary root [37], while *BIGE1* (Big embryo 1) identifies a class of genes that regulate lateral organ initiation and results in increased leaf and lateral root number [38].

The aim of this work was to establish the limiting factor in the *lpa1-1* mutant under drought stress, by analyzing and collecting parameters both on the hypogeal and epigeal parts of the plant. We compared *lpa1-1* to a wild phenotype using different approaches, spanning from hydroponics to the greenhouse.

2. Materials and Methods

2.1. Plant Materials and Controlled Growth Conditions

The *lpa1-1* mutation introgressed in B73 inbred line was kindly provided by Dr. Victor Raboy, USDA ARS, Aberdeen, ID, USA. B73 inbred line was provided by the germplasm bank at DISAA, Department of Agricultural and Environmental Sciences—Production

Landscape, Agroenergy, University of Milan. All procedures were performed in accordance with the relevant guidelines and regulations.

The first experiment was conducted in controlled conditions. Forty seeds of each genotype (B73 and the relative mutant *lpa1-1*) were sterilized with 5% (*v*/*v*) sodium hypochlorite for 15 min and then rinsed in sterile distilled water. Seeds were germinated in a Plexiglas tank covered with sheets of moistened germinating paper in a growth chamber (16 h light/8 h dark) with controlled temperature (22 °C night/28 °C day) and with photon fluence of 270 µmol m^{-2} s^{-1}. At 5 DAS (days after sowing), different parameters were measured: coleoptile length (mm), primary root length (mm), and total number of roots (primary and seminals). After one week, twelve seedlings for each genotype were transferred to hydroponics tanks containing Hoagland nutrient solution [42]. Seedlings were sampled at 16 DAS and several hypogeal and epigeal parameters were collected: shoot length (cm), shoot diameter (mm), dry weight (mg), primary root length (cm), area (cm^2), and area/L (cm^2/cm). In particular, the roots of each sample were scanned (with high-resolution digital scanner) and the images were processed using Adobe Photoshop software: the shadows of the roots and the background of the images were removed, the color of the roots was changed (green) and made uniform. The processed images were analyzed using ImageJ 1.52 [43] and Easy Leaf Area software [44] in order to collect the following data (referring to each plant): maximum root length and root system area. In addition, the root area/root length ratio was calculated.

2.2. Greenhouse Experiment

Two experiments were conducted successively in the greenhouse at the University of Milan, Italy. The temperature of day/night was 25/18 °C and the relative humidity was 60–70%. In each experiment, three plants per genotype were grown in mesocosms (13.5 cm × 100 cm, top diameter × height) filled with sandy soil (Green Maxx, VitaFlor) to 10.0 cm from the top. A layer of expanded clay was added to the base. Pots were built using transparent PVC sheets to better access the root system. The cylindrical pots were arranged randomly and three replications for each genotype were performed. To avoid exposure to light, the mesocosms were covered with a cloth. Two days before sowing, each cylinder was irrigated with 4 L of water. Each pot was sown with three seeds and then thinned to a single seedling after 10 DAS. Root growth was measured weekly and three agronomic parameters were collected in both genotypes: plant height, ear height, and culm diameter. Plants were grown until flowering using the same amount of water (1 L every week) and urea (2.5 g per plant). Finally, plants were uprooted, thoroughly washed, and subjected to phenotyping.

2.3. Leaf Temperature, Chlorophyll a Fluorescence, Stomata Opening, and Water Loss

In the mesocosms experiment, thermal images of the fifth fully expanded leaves were taken from 60-day-old *lpa1-1* and wild-type seedlings with a semiautomated long-wave infrared camera system (FLIR T650sc) in the greenhouse. Photos were taken between 11 a.m. and 12 a.m. The temperature of the leaves was then measured using the FLIR ResearchIR Max software.

Chlorophyll a fluorescence was measured using a hand-portable Handy PEA fluorimeter (Hansatech Instruments Ltd., King's Lynn, UK): leaves were dark-adapted for 30 min using the equipped white leaf-clips and fluorescence was induced by three high-intensity light-emitting diodes for one second at the maximal photosynthetic photon flux density (PPFD) of 3500 µmol m^{-2} s^{-1} [45,46]. Among all the parameters measured with the fluorimeter, Fv/Fm is widely considered a sensitive indicator of plant photosynthetic performance and represents the maximum quantum efficiency of photosystem II [47]. The performance index (PI) is essentially an indicator of sample vitality, while Dio/CS represents the energy dissipation of photosystem II.

Using clear nail varnish is a traditional method to measure stomatal density and opening. It is used to take an impression of the leaf which is then viewed under the optical

microscope. After preparing an epidermal impression by coating the leaf surface with nail varnish, the dried layer of nail varnish was removed using sellotape and finally applied on to a slide. Representative images of the stomata were taken on the fifth fully expanded leaf in the wild-type and *lpa1-1* mutant plants after 60 DAS. The ratio between the long side and the short side of the stoma was used as an indication about the shape of the stoma and its opening: the higher the ratio, the more elongated the shape; vice versa, if the ratio was close to 1, the stoma had a circular shape.

Another experiment in 15 cm pots was set up to determine the time course of the leaf water loss. After 20 days, six plants per genotype were sampled and the third leaf of each seedling was detached and weighed immediately. Leaf weight was then estimated at designated time intervals and water loss was calculated as the percentage of fresh weight based on the initial weight. Significant differences between the wild-type and *lpa1-1* were assessed by Student's *t*-test.

2.4. ICP-MS Analysis

For the ionomic analysis, seeds of the pure line B73 and the *lpa1-1* mutant were grown on moistened germination paper under controlled conditions, and the coleoptiles and seedlings were sampled at 7 and 14 DAS, respectively, before being dried at 70 °C for two days. Then, 10 mL of HNO_3 (65%) was added to 300 mg of maize dry matter in Teflon tubes. Samples were digested using a microwave digestor system (Anton Paar Multiwave 3000, Austria) in Teflon tubes applying a two-step power ramp (400 W in 5 min, maintained for 10 min; 1000 W in 10 min, maintained for 15 min). The mineralized samples were transferred into polypropylene tubes, diluted 1:40 with Milli-Q water, and element concentrations measured by ICP-MS (Varian 820 ICP- MS, Agilent, Santa Clara, CA, USA). An aliquot of 2 mg L^{-1} internal standard solution (6LI, 45Sc, 89Y, and 159Tb) was added to the samples and calibration curve to reach a final concentration of 20 $\mu g L^{-1}$.

2.5. RNA, cDNA Preparation, and Quantitative Gene Expression Analysis

RNA extraction was performed on *lpa1-1* and wild-type roots at 3 and 8 days after germination, homogenizing 100 mg of roots in liquid nitrogen. Total RNA was extracted using the Gene JET Plant RNA Purification Mini Kit (Thermo Scientific, Waltham, MA, USA) and treated with Turbo DNA-free Kit (Invitrogen, Waltham, MA, USA) according to the manufacturer's instructions. First strand cDNA was synthesized with the Maxima First Strand cDNA Synthesis (Thermo Scientific), according to the manufacturer's instructions. First strand cDNA was used as the template for subsequent PCR amplification.

Specific primers for the *orange pericarp-1* (*orp-1*) gene, which encodes the b-subunit of tryptophan synthase, was used to standardize the concentration of the samples [48]. The *orp-1* specific sequences were amplified using the following primers: forward 5′-AAGGACGTGCACACCGC-3′ and reverse 5′-CAGATACAGAACAACAACTC-3′, generating a 207 bp amplicon. A set of specific primers for root genes (*rtcs*, *rtcl*, *rum1,* and *BIGE1*) was selected from previous works [38,39,49]. The gene-specific primers are listed in Supplemental Table S1. The reaction mix underwent an initial denaturation step at 94 °C for 2 min, 32 cycles of denaturation at 94 °C for 45 s, annealing at the specific primer temperature for 1 min, and extension at 72 °C for 1 min and 30 s. Final extension at 72 °C for 5 min was performed to complete the reaction. Amplification products were visualized on 1% (*w*/*v*) agarose gels with ethidium bromide staining.

3. Results

3.1. lpa1-1 Alters RSA in Hydroponics

Under controlled conditions, the *lpa1-1* mutant appeared to grow faster in the early stages after germination compared to the control line (Figure 1). Seeds were germinated on moistened paper, and after 5 days, *lpa1-1* showed higher values than B73 control line both in the coleoptile length (29.53 vs. 18.18 mm) and in the length of the primary root

(56.35 vs. 35.13 mm) (Figure 2A,B). Furthermore, the total number of roots (primary and seminals) present in the mutant was statistically higher than in the control (Figure 2C).

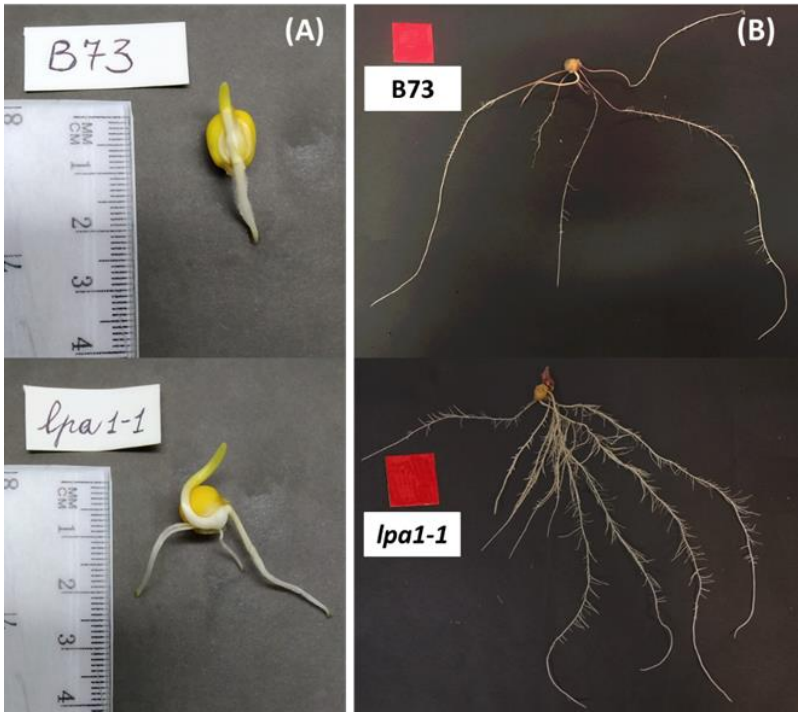

Figure 1. Representative phenotype of wild-type (B73) and *lpa1-1* at 5 DAS (**A**) and at 16 DAS, after growing in hydroponic solution (**B**).

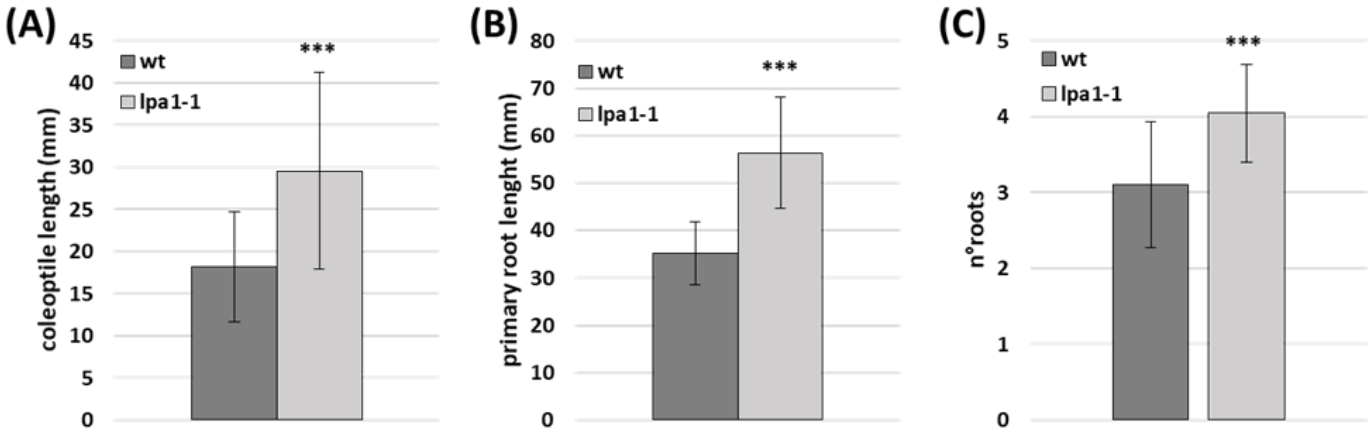

Figure 2. Coleoptile length (**A**), primary root length (**B**), and number of roots (primary and seminals) (**C**) measured at 5 DAS in controlled conditions. The data represent the mean of thirty-eight and twenty-three biological replicates for wild-type and *lpa1-1* homozygous plants, respectively. Significant differences between wild-type and *lpa1-1* were assessed by Student's *t*-test (*** $p < 0.01$).

After one week, twelve seedlings for each genotype were transferred to hydroponics, and several epigeal and hypogeal parameters were measured at 16 DAS, as shown in Figure 3.

Regarding the epigeal measurements, *lpa1-1* showed statistically higher values both in the length of the coleoptile (Figure 3A) and in the diameter of the culm (Figure 3B). Considering the root system architecture, no significant differences were found in the length of the primary roots between the two genotypes (Figure 3D); in contrast, the dry weight (DW) of the mutant root system was twice that of B73 (Figure 3C) and the area occupied by the entire root system reached 12.8 cm^2 in *lpa1-1* compared to the 6.10 cm^2 of the control

line (Figure 3E). Another parameter measured was the root area per unit of length: this ratio was statistically higher in the mutant than in the wild-type (0.55 vs. 0.28 cm^2/cm) (Figure 3F).

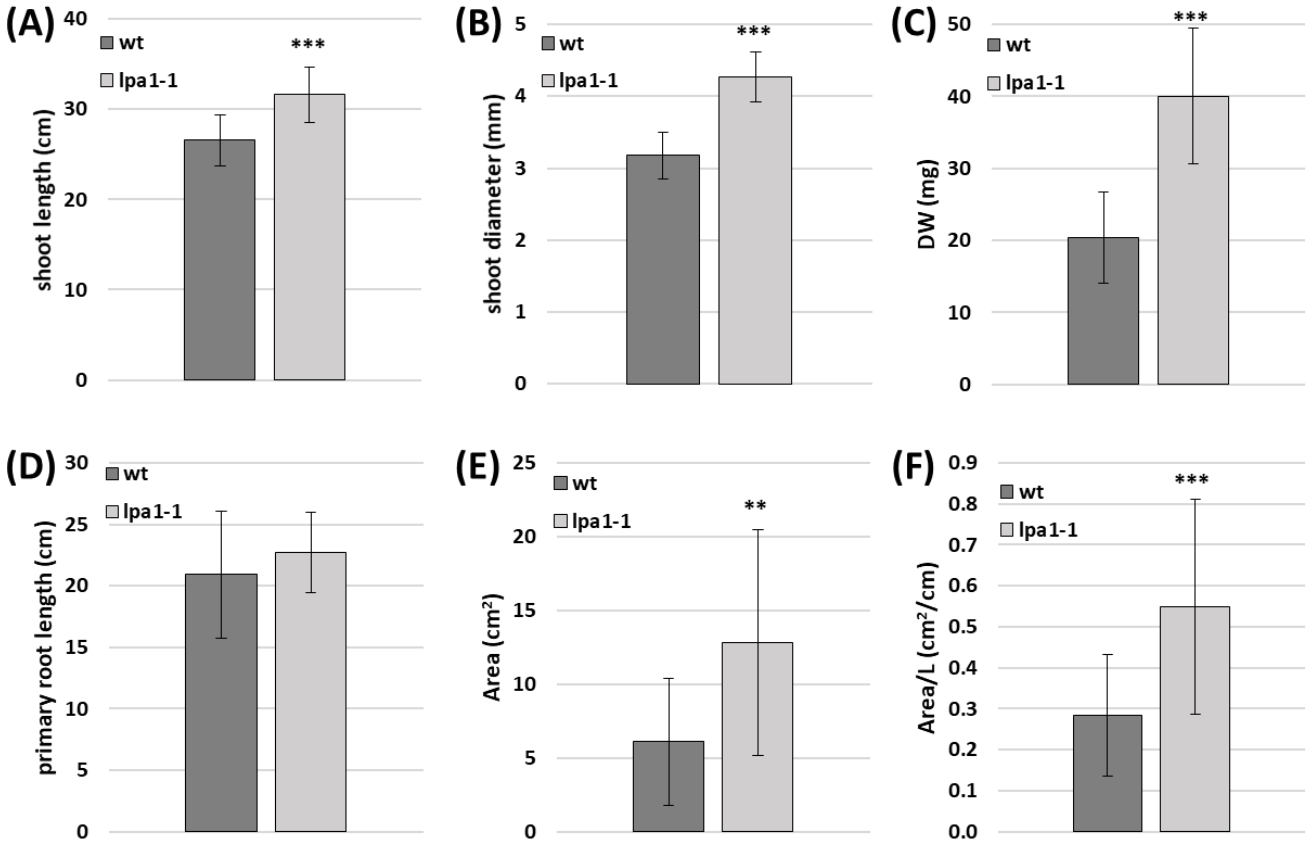

Figure 3. Measurements on the epigeal part of the plant in hydroponics at 16 DAS: shoot length (**A**) and shoot diameter (**B**). Parameters measured on the root system architecture: dry weight, DW (**C**), primary root length (**D**), area occupied by the roots (**E**), and root area per unit of length (**F**). Values represent the mean of twelve biological replicates. Significant differences between wild-type and *lpa1-1* were assessed by Student's *t*-test (** $p < 0.05$ and *** $p < 0.01$).

In the light of these data, we hypothesized that the greater bioavailability of minerals in *lpa1-1* mutant, in the early stage of development, resulted in quicker development of seedlings than in the wild-type.

Hence, the mineral and trace element content were also determined in the early stages of growth by means of ICP-MS analysis. The results showed several differences among the ion compositions of wild-type and *lpa1-1* at two sampling points, 7 and 14 DAS. In the first sampling, phosphorus was statistically more abundant in the mutant (Figure 4). In addition, other cations, such as Na, Mg, Al, K, Ca, and Se, were accumulated in higher amounts in *lpa1-1* compared to the wild phenotype (Table 1). However, at 14 DAS the mutant P content had decreased dramatically and was higher in the wild-type (Figure 4). Similarly, some minerals and trace elements that were previously more abundant in the mutant, at 14 DAS were more available in the control line (Table 1).

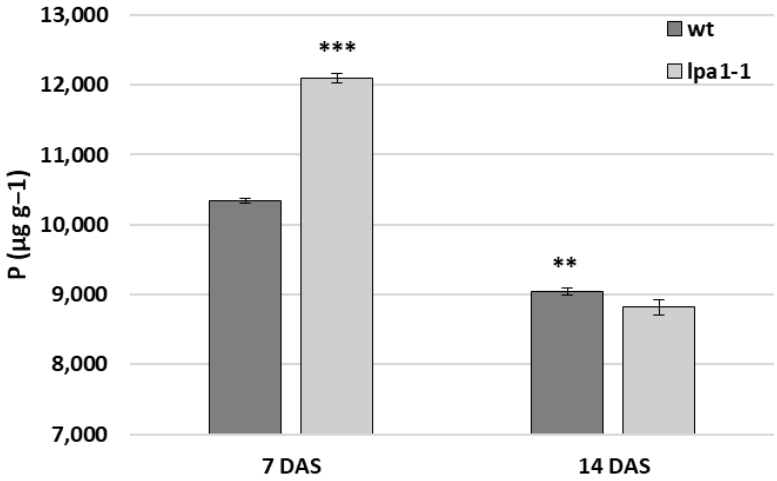

Figure 4. Phosphorus (P) content determined by inductively coupled plasma mass spectrometry (ICP-MS). Analysis performed on maize seedling dry matter of wild-type and *lpa1-1* mutant at 7 and 14 DAS. P content was expressed as micrograms per gram of dry matter. Values represent the mean of three biological replicates. Significant differences between wild-type and *lpa1-1* were assessed by Student's *t*-test (** $p < 0.05$ and *** $p < 0.01$).

Table 1. Mineral nutrient and trace element content determined by inductively coupled plasma mass spectrometry (ICP-MS). Analyses were performed on maize seedling dry matter of wild-type and *lpa1-1* mutant at 7 and 14 DAS. The elements were expressed as micrograms per gram of dry matter. SD is shown (n =3, $p < 0.05$).

	7 DAS		14 DAS	
	wt	***lpa1-1***	**wt**	***lpa1-1***
Na	311.77 ± 11.84	650.68 ± 16.21 [a]	135.67 ± 6.66	182.72 ± 22.04 [a]
Mg	2307.66 ± 36.44	2445.65 ± 12.82 [a]	2252.27 ± 57.86	2142.91 ± 26.65 [a]
Al	29.64 ± 8.35	83.25 ± 15.69 [a]	42.22 ± 5.02	47.38 ± 6.14
K	25,511.38 ± 377.77	32,858.76 ± 279.07 [a]	28,154.83 ± 533.08	27,422.72 ± 373.22
Ca	806.69 ± 12.57	881.08 ± 39.03 [a]	3252.48 ± 45.87	3314.33 ± 48.74
Cr	0.46 ± 0.03	0.72 ± 0.14 [a]	2.02 ± 0.26	1.40 ± 0.19 [a]
Mn	9.16 ± 0.31	8.23 ± 0.09 [a]	21.78 ± 1.15	18.44 ± 0.03 [a]
Fe	78.89 ± 6.31	74.63 ± 19.58	128.89 ± 1.86	134.45 ± 24.29
Cu	7.66 ± 1.18	10.15 ± 2.76	7.30 ± 1.03	8.72 ± 1.64
Zn	140.88 ± 3.44	119.18 ± 5.55 [a]	103.96 ± 3.47	93.35 ± 3.81 [a]
Se	0.69 ± 0.02	1.60 ± 0.08 [a]	0.87 ± 0.18	1.60 ± 0.38 [a]

[a] Statistically different from wt, based on *t*-test.

3.2. Root Genes Involved in Auxin Signal Transduction

The content of minerals and trace elements gives us indications of the rapid development of the mutant in the early stages of growth but does not explain the different root systems between the mutant and the control line. These differences in the mutant RSA could be attributable to an alteration in the polar transport of auxins: it is known that inositol phosphates are involved in the polar transport of auxins, important phytohormones that regulate several plant developmental processes and responses to environmental stresses [50,51]. In this work we selected four genes involved in auxin signal transduction that are key elements for the development of seminal, lateral, and shoot-borne roots in maize: *rtcs1* (accession number Zm00001eb003920), *rtcl1* (Zm00001d048401), *rum1* (Zm00001eb156910), and *BIGE1* (Zm00001eb211050) gene expression levels were analyzed on 3- and 8-day roots of wild-type and *lpa1-1* by reverse transcription polymerase chain reaction (RT-PCR) (see "Materials and Methods" for details). As shown in Figure 5, *rtcs1* was upregulated in *lpa1-1* roots at 8 DAS compared to the wild-type corresponding tissues, but this difference was

lower at the 3-day sampling. A similar pattern was observed for its paralog, *rtcl1 (rtcs-like)*, even if the expression at 8 DAS was reduced, and *rum1* showed no differences in expression levels between the two genotypes in either sampling. Moreover, *BIGE1* was upregulated at 8 DAS in the mutant roots than in the wild-type, while these differences were not found at 3 days (Figure 5).

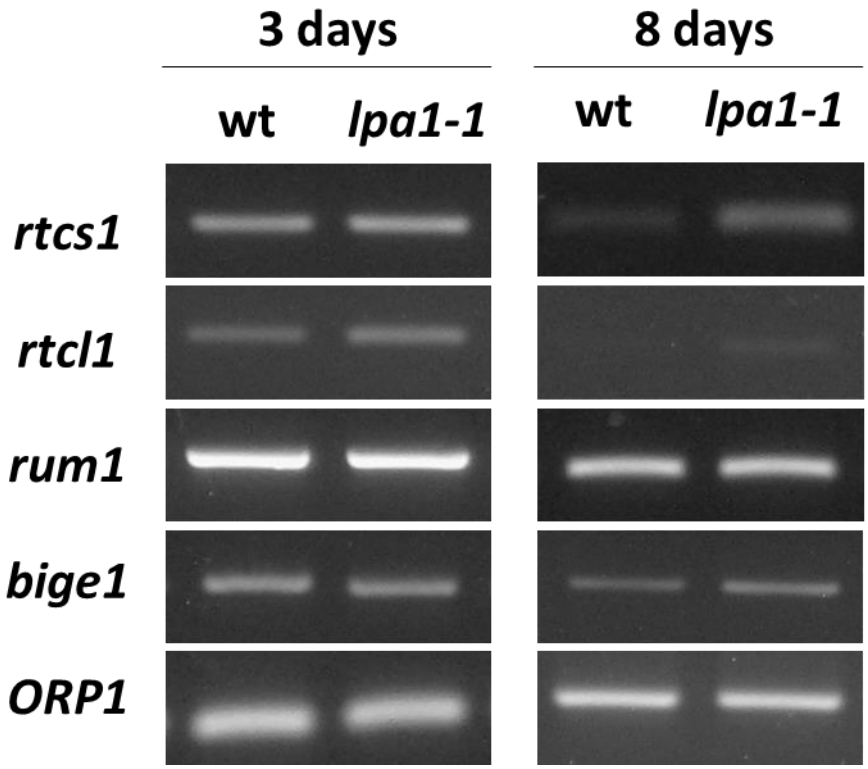

Figure 5. *rtcs1*, *rtcl1*, *rum1* and *bige1* gene expression levels on 3- and 8-day roots of wild-type and *lpa1-1*. *Orp1* gene was used as control.

3.3. Root Depth Is Not Affected in lpa1-1

In the mesocosms experiment, the growth of the embryonic primary root and the post-embryonic crown roots was monitored weekly to understand if a different root depth was the main cause of the drought stress observed in *lpa1-1* mutant. In the first replicate, the primary root of the mutant did not differ significantly from the wild phenotype at any of the four points of detection (Figure 6A). In the second replicate of the experiment, no significant differences were found, except at 36 DAS, in which *lpa1-1* roots were statistically deeper than those of the control (67.83 vs. 54.67 cm, respectively) (Figure 6A). Considering the growth of the post-embryonic crown roots, in the two experiments there were no significant differences in crown root depth, except for the measurement at 64 DAS in the first trial (Figure 6B). Furthermore, the dry weight of the entire root system measured after the final cleaning was statistically the same in both the experiments (data not shown).

Different epigeal parameters were collected on plants grown in mesocosms: the mutant showed a reduced plant and ear height compared to the pure line in most of the samplings (Figure 7A,B). Moreover, the plant culm diameter was measured weekly using an electronic caliper: in both the experiments, culm diameter was higher in the mutant, but the difference was statistically significant at few sampling points (Figure 7C).

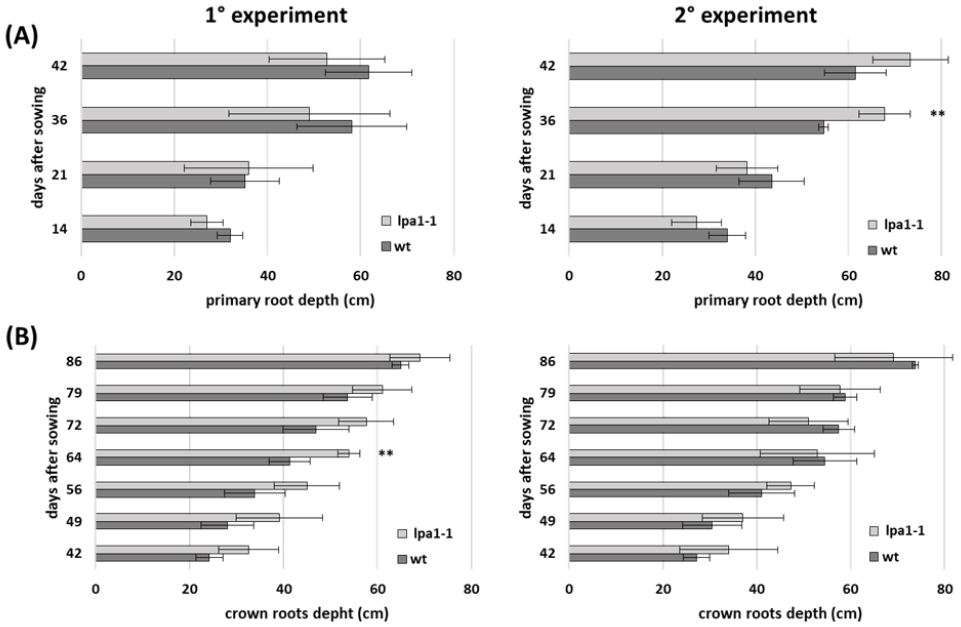

Figure 6. Depth of the embryonic primary root (**A**) and of the post-embryonic crown roots (**B**) measured every week till flowering. The data represent the means of three biological replicates in two different experiments. Significant differences between wild-type and *lpa1-1* were assessed by Student's *t*-test (** $p < 0.05$).

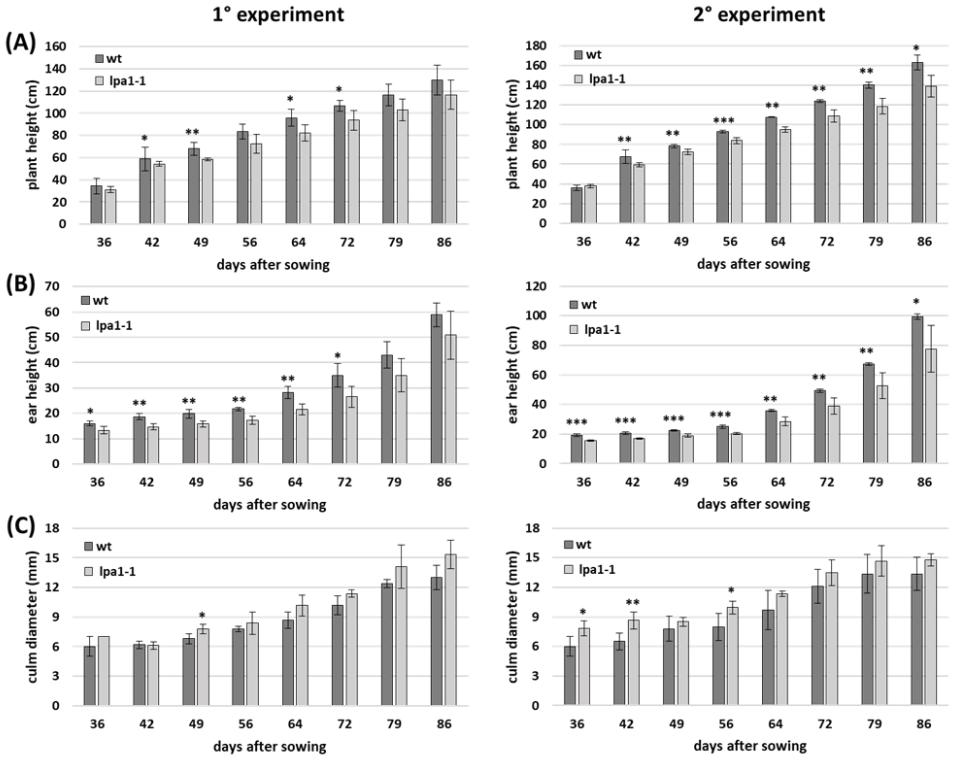

Figure 7. Plant height (**A**), ear height (**B**), and culm diameter (**C**) measured every week till flowering in two different experiments. The data represent the means of three biological replicates. Significant differences between wild-type and *lpa1-1* were assessed by Student's *t*-test (* $p < 0.1$, ** $p < 0.05$, and *** $p < 0.01$).

3.4. Cuticular Permeability Is Altered in lpa1-1 Mutant

The results obtained so far seem to exclude the root system as the main cause of the drought stress in *lpa1-1*. Hence, our research focused on the aerial part of the plant, and several measurements were carried out.

In order to investigate the impact of drought stress on the mutant, thermography images of the fifth fully expanded leaves of wild-type and *lpa1-1* homozygous mutant were analyzed (Figure 8A). In both the experiments, *lpa1-1* presented a reduced leaf temperature compared to the control (Figure 8B), probably due to a greater water loss from stomata. For this reason, the photos of the stomata were taken with the optical microscope (Figure 8C). The subsequent analysis allowed the calculation of the ratio between the long side and the short side of the stoma. This parameter gave us an indication about the shape of the stoma and its opening: the higher the ratio, the more elongated the shape; conversely, if the ratio was close to 1, the stomata had a circular shape. The stomata of the wild phenotype were characterized by a statistically higher ratio in the two experiments, and, consequently, by a more elongated shape (Figure 8D). In contrast, the stomata of the mutant had a lower ratio and a circular shape, which could cause greater water loss under stressful conditions.

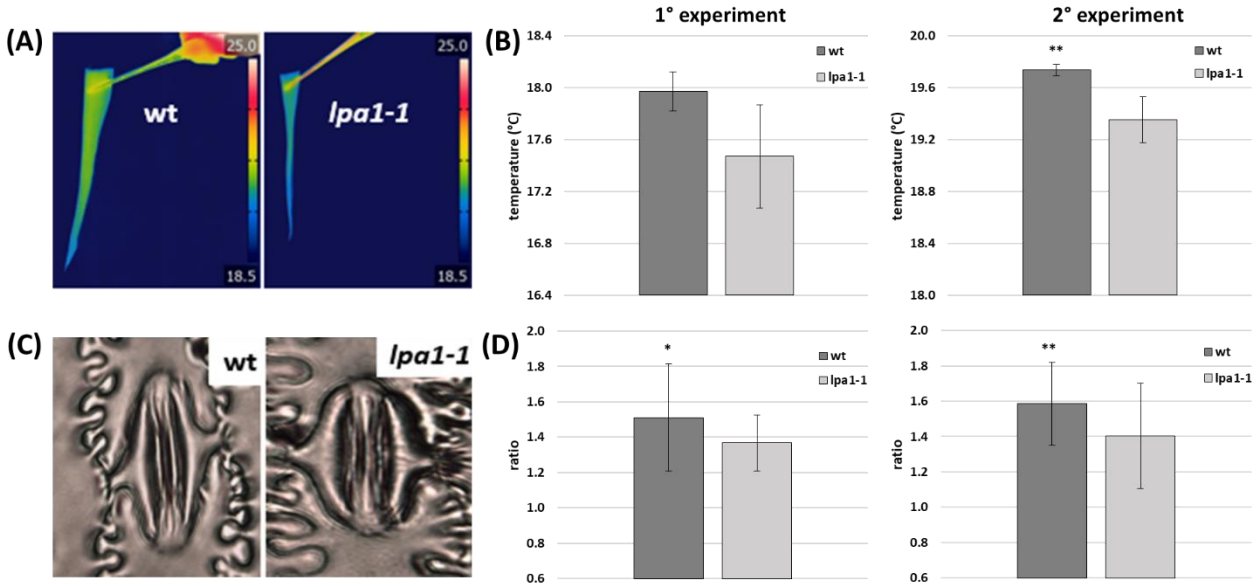

Figure 8. (**A**) Representative images of the leaf temperature acquired with the thermographic camera (FLIR T650sc) in wild-type and homozygous *lpa1-1* plants. (**B**) Temperature of the fifth fully expanded leaf in the wild-type and *lpa1-1* homozygous plants measured at 60 days after sowing (DAS). Values represent the mean of three biological replicates in two different experiments. Significant differences between wild-type and *lpa1-1* were assessed by Student's *t*-test (* $p < 0.1$ and ** $p < 0.05$). (**C**) Representative images of the stoma acquired by optical microscope on the fifth fully expanded leaf in wild-type and *lpa1-1* mutant plants at 60 DAS. (**D**) Ratio between the long side and the short side of the stoma. This parameter gives us an indication about the shape of the stoma and its opening: the higher the ratio, the more elongated the shape; if the ratio is close to 1, the stoma has a circular shape. Values represent the mean of eighteen biological replicates. Significant differences between wild-type and *lpa1-1* were assessed by Student's *t*-test (* $p < 0.1$ and ** $p < 0.05$).

Hence, it seems that the mutant plant suffers more from drought stress compared to the control line. Consequently, the efficiency of photosystem II measured with the fluorometer should also decrease. The parameter Fv/Fm represents the maximum quantum efficiency of PSII and gives information on the potential photosynthetic ability of the plant. In both the experiments, the mean was around 0.810 in the wild phenotype, while it was lower, at 0.800, in *lpa1-1* mutant (Figure 9A). The performance index (PI) had a similar trend to Fv/Fm ratio: the graphs show a statistically significant difference ($p < 0.05$) with higher values in the control line compared to the mutant (Figure 9B). In particular, the values of

P.I. in the control line were higher than those of the mutant by 22.5% and 20.7% in the two experiments. On the other hand, the parameter Dio/CS measured with the same fluorimeter represents the energy dissipation of photosystem II. The results showed that *lpa1-1* lost more energy than the wild-type, supporting the hypothesis that the mutant is characterized by a lower photosynthetic efficiency (Figure 9C).

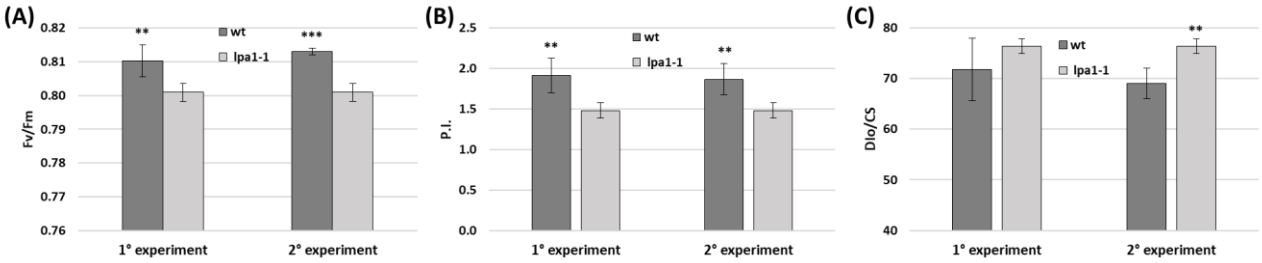

Figure 9. The fluorimeter Handy PEA+ was used to measure Fv/Fm (**A**) and other important photosynthetic parameters, such as the performance index (PI) (**B**) and the energy dissipation of photosystem II (Dio/CS) (**C**). Values represent the mean of three biological replicates. Significant differences between wild-type and *lpa1-1* were assessed by Student's *t*-test (** $p < 0.05$ and *** $p < 0.01$).

Moreover, to better understand the impact of the mutation *lpa1-1* on leaf surface permeability, a water loss time course experiment was carried out on the third detached leaf by estimating the loss of weight with respect to the initial leaf fresh weight. The resulting profiles showed that *lpa1-1* was characterized by a higher water loss rate compared to wild-type plants (Figure 10).

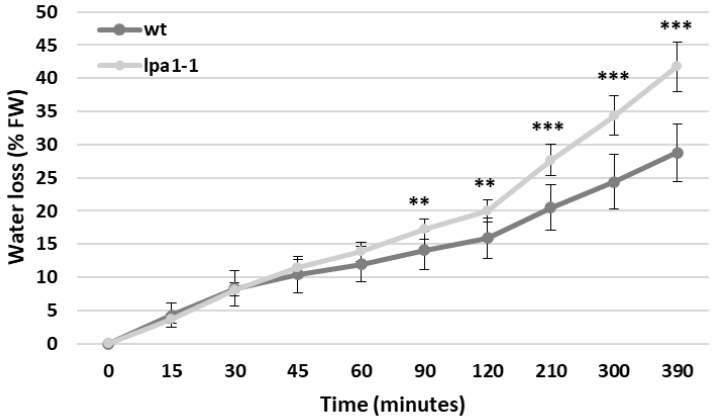

Figure 10. Percentage of water loss in the third detached leaf of homozygous *lpa1-1* and wild-type. Values represent the mean of six biological replicates. Significant differences between wild-type and *lpa1-1* were assessed by Student's *t*-test (** $p < 0.05$ and *** $p < 0.01$).

4. Discussion

Phytic acid is considered an anti-nutritional factor for human and monogastric animals and it is also involved in environmental problems of phosphorus pollution. In underdeveloped countries, the lack of important cations such as iron and zinc in the diet represents a serious problem for human health. On the other hand, in rich countries the problem is not nutritional, but related to feed: farmers must supply mineral phosphorus to the feed of monogastric animals, thus increasing the cost [5].

In the past few years, some programs have analyzed the genetic variability of both phytic acid and inorganic phosphorus present in different accession collected in the germplasm bank [8,9]. Lorenz and colleagues reported that the phosphorus fraction of wild maize grains could be modified by breeding and selection, demonstrating that the phytic acid–phosphorus and, consequently, the mineral nutrients' accumulations are controlled by several QTLs [9]. However, in this context, the most promising strategy concerns the

use of *low phytic acid* (*lpa*) mutants. The *lpa* trait can provide several potential benefits to the nutritional quality of foods and feeds and to the environmental P sustainability in agriculture [52].

In maize, four different *lpa1* mutants have been isolated and characterized so far, and *lpa1-1* is the most promising. However, reducing PA content in seeds to improve nutritional quality affects seed quality and plant performance, as recently reviewed by Colombo and coworkers [29]. Among these pleiotropic effects, a greater susceptibility to drought stress was observed in the field on *lpa1-1*, and our recent research focused on this agronomic defect.

In fact, in recent decades, low water availability is considered a primary limitation to crop productivity all around the world [53,54]. The frequency and the severity of drought stress on crops will increase in the future because of climate change [55]. The greater water loss observed in *lpa1-1* could be caused by an alteration in root system architecture or by differences in the aerial part of the plant. The aim of this work was to establish which was the limiting factor in the mutant *lpa1-1*, analyzing and collecting parameters on both the hypogeal and epigeal parts of the plant.

Regarding the root system architecture, many differences were found between the mutant and the wild-type phenotype (Figure 1). From the data measured after 5 days on wet paper, a greater development of the mutant was observed compared to the pure line B73 (Figures 1A and 2B,C). The fast growth of *lpa1-1* in the first weeks after germination was also confirmed at 16 DAS, after the transfer of the seedlings to hydroponics (Figure 1B). Once again, the mutant's root system appeared more developed: both the dry weight and the root area per unit of length were twice that of B73 (Figure 3C,F). These differences in the mutant root system could be attributable to an alteration in the polar transport of auxins. In fact, several studies carried out on different species have shown that inositol phosphates are involved in the polar transport of auxins, important phytohormones that regulate numerous plant developmental processes and responses to environmental stress [50,51]. For instance, a previous study on Arabidopsis reported that null mutations in the inositol–phosphate synthase *MIPS1* gene had dramatic impacts on plant development, including impaired embryogenesis and altered cotyledon development, root agravitropism, reduced transport of auxin, and altered root cap organization [56].

Furthermore, another factor that could influence the faster growth of *lpa1-1* is the higher bioavailability of phosphorus and minerals in the early stages of development (Table 1, Figure 4). Similar measurements at ICP-MS were previously carried out on seeds by Landoni et al. [57]. In this work, these analyses were conducted for the first time on seedlings. These results confirmed a strong chelating effect of PA on mineral cations in the control line, while the *lpa1-1* mutant was characterized by more bioavailable cations that do not need to be released gradually by the phytase enzyme.

At this point, since the root architecture did not appear to be a limiting factor, we thought that drought stress in the field could be caused by different root depths. Root depth plays a central role in plant resistance to water stress [58,59]. In order to analyze this trait, plants were grown in transparent mesocosms. The use of mesocosms allowed the control of different conditions, such as soil type and moisture, temperature, light intensity, pot sizes, and nutrient and water inputs [60]. From the data collected weekly, it emerged that in the two experiments there were no significant differences (except at a few sampling points) either in the depth of the embryonic primary root (Figure 6A) or in that of post-embryonic crown roots (Figure 6B).

Therefore, the experiments conducted in this work showed for the first time that root depth did not appear to be the main cause of the drought stress observed on *lpa1-1* mutant plants in the field, even if the RSA showed many differences in the two genotypes. In particular, the mutant root system was characterized by a greater development in the first weeks after germination: the higher dry weight and the larger root surface recorded in hydroponics seemed to be determined by early lateral root and root hair development.

For this reason, from the literature we selected many root genes involved in auxin signal transduction that are fundamental for the development of lateral, seminal, and shoot-borne roots [40]. Expression analysis carried out on 3- and 8-day roots of wild-type and *lpa1-1* revealed the high abundance of *rtcs* transcripts in the mutant, in line with the role of this gene. The upregulation of *rtcs* in mutant plants suggested an alteration in the polar transport of auxins. In the same way, expression analysis on *BIGE1* (involved in lateral organ initiation) confirmed the upregulation of *BIGE1* transcripts at 8 days.

Despite this possible alteration in the auxin polar transport, the root system was excluded as the main cause of the drought stress, and so our research focused on the aerial parts of the plant. Epigeal data collected at 5 and 16 DAS in the experiment performed under controlled conditions confirmed the faster development of *lpa1-1* in the early stages (Figures 1A and 2A,B). In fact, due to the reduction of phytic acid in *lpa* mutants, the cations are more bioavailable, while in the wild phenotype they tend to form phytate salts. The situation changed completely after two weeks: the seedling phosphorus content decreased dramatically in the mutant (Figure 4), and several minerals (previously more abundant in *lpa1-1*) were more abundant in the control line (Table 1). The measurements carried out in the mesocosms experiment on the aerial parts of the plant confirmed this hypothesis: after a few weeks, the agronomic performance of B73 improved significantly and some important parameters (such as plant height and ear height) were statistically higher at most of the sampling points in both the experiments (Figure 7A,B). The shortening of the internodes found in *lpa1-1* plants and the increased culm diameter (Figure 7C) could be caused by an alteration in the polar transport of the auxins. In fact, some known maize mutants, such as *brachytic 2* (*br2*) and *brevis plant1* (*bv1*), are characterized by shortened internodes and are deficient in auxin transport [61–63].

In the same experiment conducted in the greenhouse, several epigeal parameters were measured in both genotypes in order to understand the causes of drought stress. *Lpa1-1* exhibited reduced leaf temperature compared to its control (Figure 8A,B), possibly due to increased water loss from leaves (Figure 10). It was found that the efficiency of photosystem II measured with the Handy PEA fluorimeter was lower in mutant plants (Figure 9A,B), probably due to a greater dissipation of energy in the leaves (Figure 9C). In this context, we cannot exclude that the water loss observed in the *lpa1-1* mutant is also associated with alterations in the cuticle and/or cell wall composition. In fact, both cuticular waxes and lignin constitute a natural protection against damage caused by biotic and abiotic factors, as well as a waterproof barrier that regulates water loss and leaf gas exchange [64,65].

In conclusion, further breeding work will be necessary to clarify the causes of water loss in this mutant and to attenuate the negative pleiotropic effects impacting on plant performance. The aim is to overcome these agronomic defects and exploit the potential of the *lpa* trait, especially for underdeveloped countries, where diet is based on staple crops.

In this work, the experiments were performed under controlled or semi-controlled conditions. Field tests are underway to confirm the hypothesis that drought stress is caused by a reduced photosynthetic efficiency in the *lpa1-1* mutant, and not by a shallower root system, as previously reported. In this work, the comparisons and measurements were carried out using the pure line B73. The introgression of the *lpa1-1* mutation into a new genetic background (such as commercial hybrids) could represent a solution and could improve the performance of the plant, contributing to overcome the effects of drought stress described here. Several breeding programs are in progress in order to develop new *lpa* varieties by conventional breeding and transgenic/genome editing methods. In this way it will be possible to exploit the nutritional properties of this mutant and improve the P management in agriculture.

Supplementary Materials: The following supporting information can be downloaded at: https://www.mdpi.com/article/10.3390/agronomy12030721/s1, Table S1: Gene specific primers.

Author Contributions: Conceptualization, R.P. and F.C.; Methodology, F.C.; Software, L.G.; Validation, G.B., M.G. and M.P.; Formal Analysis, F.C.; Investigation, F.C.; Resources, R.P.; Data Curation, F.C.; Writing—Original Draft Preparation, F.C.; Writing—Review and Editing, G.B.; Visualization, M.G.; Supervision, R.P.; Project Administration, R.P.; Funding Acquisition, R.P. All authors have read and agreed to the published version of the manuscript.

Funding: This research received no external funding.

Institutional Review Board Statement: Not applicable.

Informed Consent Statement: Not applicable.

Data Availability Statement: Not applicable.

Acknowledgments: We wish to thank Davide Reginelli for his hard work in the field and Lesley Currah for her editing and suggestions.

Conflicts of Interest: The authors declare no conflict of interest.

References

1. Raboy, V. *Accumulation and Storage of Phosphate and Minerals*; Larkins, B.A., Vasil, I.K., Eds.; Kluwer Academic: Dordrecht, The Netherlands, 1997.
2. O'Dell, B.L.; de Boland, A.R.; Koirtyohann, S.R. Distribution of Phytate and Nutritionally Important Elements among the Morphological Components of Cereal Grains. *J. Agric. Food Chem.* **1972**, *20*, 718–723. [CrossRef]
3. Raboy, V. Progress in Breeding Low Phytate Crops. *Am. Soc. Nutr. Sci.* **2002**, *132*, 503–505. [CrossRef] [PubMed]
4. Laboure, A.M.; Gagnon, J.; Lescure, A.M. Purification and characterization of a phytase (myo-inositol-hexakisphosphate phosphohydrolase) accumulated in maize (*Zea mays*) seedlings during germination. *Biochem. J.* **1993**, *295*, 413–419. [CrossRef] [PubMed]
5. Raboy, V. Approaches and challenges to engineering seed phytate and total phosphorus. *Plant Sci.* **2009**, *177*, 281–296. [CrossRef]
6. Graf, E.; Eaton, J.W. Antioxidant functions of phytic acid. *Free Radic. Biol. Med.* **1990**, *8*, 61–69. [CrossRef]
7. Doria, E.; Galleschi, L.; Calucci, L.; Pinzino, C.; Pilu, R.; Cassani, E.; Nielsen, E. Phytic acid prevents oxidative stress in seeds: Evidence from a maize (*Zea mays* L.) low phytic acid mutant. *J. Exp. Bot.* **2009**, *60*, 967–978. [CrossRef]
8. Lorenz, A.J.; Scott, M.P.; Lamkey, K.R. Quantitative determination of phytate and inorganic phosphorus for maize breeding. *Crop Sci.* **2007**, *47*, 600–606. [CrossRef]
9. Lorenz, A.J.; Scott, M.P.; Lamkey, K.R. Genetic variation and breeding potential of phytate and inorganic phosphorus in a maize population. *Crop Sci.* **2008**, *48*, 79–84. [CrossRef]
10. Raboy, V.; Gerbasi, P.F.; Young, K.A.; Stoneberg, S.D.; Pickett, S.G.; Bauman, A.T.; Murthy, P.P.N.; Sheridan, W.F.; Ertl, D.S. Origin and seed phenotype of maize low phytic acid 1-1 and low phytic acid 2-1. *Plant Physiol.* **2000**, *124*, 355–368. [CrossRef] [PubMed]
11. Pilu, R.; Panzeri, D.; Gavazzi, G.; Rasmussen, S.K.; Consonni, G.; Nielsen, E. Phenotypic, genetic and molecular characterization of a maize low phytic acid mutant (lpa241). *Theor. Appl. Genet.* **2003**, *107*, 980–987. [CrossRef]
12. Badone, F.C.; Amelotti, M.; Cassani, E.; Pilu, R. Study of low phytic acid1-7 (lpa1-7), a new ZmMRP4 mutation in maize. *J. Hered.* **2012**, *103*, 598–605. [CrossRef] [PubMed]
13. Borlini, G.; Rovera, C.; Landoni, M.; Cassani, E.; Pilu, R. Lpa1-5525: A new lpa1 mutant isolated in a mutagenized population by a novel non-disrupting screening method. *Plants* **2019**, *8*, 209. [CrossRef] [PubMed]
14. Guttieri, M.; Bowen, D.; Dorsch, J.A.; Raboy, V.; Souza, E. Identification and characterization of a low phytic acid wheat. *Crop Sci.* **2004**, *44*, 418–424. [CrossRef]
15. Larson, S.R.; Young, K.A.; Cook, A.; Blake, T.K.; Raboy, V. Linkage mapping of two mutations that reduce phytic acid content of barley grain. *Theor. Appl. Genet.* **1998**, *97*, 141–146. [CrossRef]
16. Rasmussen, S.K.; Hatzack, F. Identification of two low-phytate barley (*Hordeum vulgare* L.) grain mutants by TLC and genetic analysis. *Hereditas* **1998**, *129*, 107–112. [CrossRef]
17. Bregitzer, P.; Raboy, V. Effects of four independent low-phytate mutations on barley agronomic performance. *Crop Sci.* **2006**, *46*, 1318–1322. [CrossRef]
18. Larson, S.R.; Rutger, J.N.; Young, K.A.; Raboy, V. Isolation and genetic mapping of a non-lethal rice (*Oryza sativa* L.) low phytic acid 1 mutation. *Crop Sci.* **2000**, *40*, 1397–1405. [CrossRef]
19. Liu, Q.L.; Xu, X.H.; Ren, X.L.; Fu, H.W.; Wu, D.X.; Shu, Q.Y. Generation and characterization of low phytic acid germplasm in rice (*Oryza sativa* L.). *Theor. Appl. Genet.* **2007**, *114*, 803–814. [CrossRef]
20. Wilcox, J.R.; Premachandra, G.S.; Young, K.A.; Raboy, V. Isolation of high seed inorganic P, low-phytate soybean mutants. *Crop Sci.* **2000**, *40*, 1601–1605. [CrossRef]
21. Hitz, W.D.; Carlson, T.J.; Kerr, P.S.; Sebastian, S.A. Biochemical and molecular characterization of a mutation that confers a decreased raffinosaccharide and phytic acid phenotype on soybean seeds. *Plant Physiol.* **2002**, *128*, 650–660. [CrossRef]
22. Yuan, F.J.; Zhao, H.J.; Ren, X.L.; Zhu, S.L.; Fu, X.J.; Shu, Q.Y. Generation and characterization of two novel low phytate mutations in soybean (*Glycine max* L. Merr.). *Theor. Appl. Genet.* **2007**, *115*, 945–957. [CrossRef] [PubMed]

23. Campion, B.; Sparvoli, F.; Doria, E.; Tagliabue, G.; Galasso, I.; Fileppi, M.; Bollini, R.; Nielsen, E. Isolation and characterisation of an lpa (low phytic acid) mutant in common bean (*Phaseolus vulgaris* L.). *Theor. Appl. Genet.* **2009**, *118*, 1211–1221. [CrossRef] [PubMed]
24. Cominelli, E.; Confalonieri, M.; Carlessi, M.; Cortinovis, G.; Daminati, M.G.; Porch, T.G.; Losa, A.; Sparvoli, F. Phytic acid transport in Phaseolus vulgaris: A new low phytic acid mutant in the PvMRP1 gene and study of the PvMRPs promoters in two different plant systems. *Plant Sci.* **2018**, *270*, 1–12. [CrossRef] [PubMed]
25. Shi, J.; Wang, H.; Hazebroek, J.; Ertl, D.S.; Harp, T. The maize low-phytic acid 3 encodes a myo-inositol kinase that plays a role in phytic acid biosynthesis in developing seeds. *Plant J.* **2005**, *42*, 708–719. [CrossRef] [PubMed]
26. Shi, J.; Wang, H.; Schellin, K.; Li, B.; Faller, M.; Stoop, J.M.; Meeley, R.B.; Ertl, D.S.; Ranch, J.P.; Glassman, K. Embryo-specific silencing of a transporter reduces phytic acid content of maize and soybean seeds. *Nat. Biotechnol.* **2007**, *25*, 930–937. [CrossRef]
27. Pilu, R.; Landoni, M.; Cassani, E.; Doria, E.; Nielsen, E. The maize lpa241 mutation causes a remarkable variability of expression and some pleiotropic effects. *Crop Sci.* **2005**, *45*, 2096–2105. [CrossRef]
28. Pilu, R.; Panzeri, D.; Cassani, E.; Badone, F.C.; Landoni, M.; Nielsen, E. A paramutation phenomenon is involved in the genetics of maize low phytic acid1-241 (lpa1-241) trait. *Heredity* **2009**, *102*, 236–245. [CrossRef]
29. Colombo, F.; Paolo, D.; Cominelli, E.; Sparvoli, F.; Nielsen, E.; Pilu, R. MRP Transporters and Low Phytic Acid Mutants in Major Crops: Main Pleiotropic Effects and Future Perspectives. *Front. Plant Sci.* **2020**, *11*, 1–12. [CrossRef]
30. Hochholdinger, F.; Park, W.J.; Sauer, M.; Woll, K. From weeds to crops: Genetic analysis of root development in cereals. *Trends Plant Sci.* **2004**, *9*, 42–48. [CrossRef]
31. Hochholdinger, F.; Tuberosa, R. Genetic and genomic dissection of maize root development and architecture. *Curr. Opin. Plant Biol.* **2009**, *12*, 172–177. [CrossRef]
32. Sanguineti, M.C.; Giuliani, M.M.; Govi, G.; Tuberosa, R.; Landi, P. Root and shoot traits of maize inbred lines grown in the field and in hydroponic culture and their relationships with root lodging. *Maydica* **1998**, *43*, 211–216.
33. Abbe, E.C.; Stein, O.L. The Growth of the Shoot Apex in Maize: Embryogeny. *Am. J. Bot.* **1954**, *41*, 285–293. [CrossRef]
34. Hochholdinger, F.; Woll, K.; Sauer, M.; Dembinsky, D. Genetic dissection of root formation in maize (*Zea mays*) reveals root-type specific developmental programmes. *Ann. Bot.* **2004**, *93*, 359–368. [CrossRef] [PubMed]
35. Yu, P.; Gutjahr, C.; Li, C.; Hochholdinger, F. Genetic Control of Lateral Root Formation in Cereals. *Trends Plant Sci.* **2016**, *21*, 951–961. [CrossRef]
36. Taramino, G.; Sauer, M.; Stauffer, J.L.; Multani, D.; Niu, X.; Sakai, H.; Hochholdinger, F.; Suzuki, M.; Sato, Y.; Wu, S.; et al. The maize (*Zea mays* L.) RTCS gene encodes a LOB domain protein that is a key regulator of embryonic seminal and post-embryonic shoot-borne root initiation. *Plant Cell* **2007**, *27*, 2288–2300. [CrossRef] [PubMed]
37. von Behrens, I.; Komatsu, M.; Zhang, Y.; Berendzen, K.W.; Niu, X.; Sakai, H.; Taramino, G.; Hochholdinger, F. Rootless with undetectable meristem 1 encodes a monocot-specific AUX/IAA protein that controls embryonic seminal and post-embryonic lateral root initiation in maize. *Plant J.* **2011**, *66*, 341–353. [CrossRef]
38. Suzuki, M.; Sato, Y.; Wu, S.; Kang, B.H.; McCarty, D.R. Conserved functions of the MATE transporter BIG EMBRYO1 in regulation of lateral organ size and initiation rate. *Plant Cell* **2015**, *27*, 2288–2300. [CrossRef]
39. Xu, C.; Tai, H.; Saleem, M.; Ludwig, Y.; Majer, C.; Berendzen, K.W.; Nagel, K.A.; Wojciechowski, T.; Meeley, R.B.; Taramino, G.; et al. Cooperative action of the paralogous maize lateral organ boundaries (LOB) domain proteins RTCS and RTCL in shoot-borne root formation. *New Phytol.* **2015**, *207*, 1123–1133. [CrossRef]
40. Hochholdinger, F.; Yu, P.; Marcon, C. Genetic Control of Root System Development in Maize. *Trends Plant Sci.* **2018**, *23*, 79–88. [CrossRef]
41. Hetz, W.; Hochholdinger, F.; Schwall, M.; Feix, G. Isolation and characterization of rtcs, a maize mutant deficient in the formation of nodal roots. *Plant J.* **1996**, *10*, 845–857. [CrossRef]
42. Hoagland, D.R.; Arnon, D.I. The Water-Culture Method for Growing Plants without Soil. *Circ. Calif. Agric. Exp. Stn.* **1950**, *347*, 1–32.
43. Schneider, C.A.; Rasband, W.S.; Eliceiri, K.W. NIH Image to ImageJ: 25 years of image analysis. *Nat. Methods* **2012**, *9*, 671–675. [CrossRef] [PubMed]
44. Easlon, H.M.; Bloom, A.J. Easy Leaf Area: Automated digital image analysis for rapid and accurate measurement of leaf area. *Appl. Plant Sci.* **2014**, *2*, 1400033. [CrossRef] [PubMed]
45. Strasser, R.J.; Srivastava, A.; Tsimilli-Michael, M. The fluorescence transient as a tool to characterize and screen photosynthetic samples. In *Probing Photosynthesis Mechanism, Regulation & Adaptation*; CRC Press: Boca Raton, FL, USA, 2000; pp. 443–480.
46. Giorio, P. Black leaf-clips increased minimum fluorescence emission in clipped leaves exposed to high solar radiation during dark adaptation. *Photosynthetica* **2011**, *49*, 371–379. [CrossRef]
47. Strasser, R.J.; Tsimilli-Michael, M.; Srivastava, A. *Analysis of the Fluorescence Transient*; Advances in Photosynthesis and Respiration Series 19; Springer: Berlin/Heidelberg, Germany, 2004; ISBN 9781402032189.
48. Wright, A.D.; Moehlenkamp, C.A.; Perrot, G.H.; Gerald Neuffer, M.; Cone, K.C. The maize auxotrophic mutant orange pericarp is defective in duplicate genes for tryptophan synthase β. *Plant Cell* **1992**, *4*, 711–719. [CrossRef]
49. Zhang, Y.; Paschold, A.; Marcon, C.; Liu, S.; Tai, H.; Nestler, J.; Yeh, C.-T.; Opitz, N.; Lanz, C.; Schnable, P.S.; et al. The Aux/IAA gene rum1 involved in seminal and lateral root formation controls vascular patterning in maize (*Zea mays* L.) primary roots. *J. Exp. Bot.* **2014**, *65*, 4919–4930. [CrossRef]

50. Woodward, A.W.; Bartel, B. Auxin: Regulation, action, and interaction. *Ann. Bot.* **2005**, *95*, 707–735. [CrossRef]
51. Teale, W.D.; Paponov, I.A.; Palme, K. Auxin in action: Signalling, transport and the control of plant growth and development. *Nat. Rev. Mol. Cell Biol.* **2006**, *7*, 847–859. [CrossRef]
52. Sparvoli, F.; Cominelli, E. Seed biofortification and phytic acid reduction: A conflict of interest for the plant? *Plants* **2015**, *4*, 728–755. [CrossRef]
53. Lynch, J.P. Roots of the second green revolution. *Aust. J. Bot.* **2007**, *55*, 493–512. [CrossRef]
54. Lobell, D.B.; Roberts, M.J.; Schlenker, W.; Braun, N.; Little, B.B.; Rejesus, R.M.; Hammer, G.L. Greater sensitivity to drought accompanies maize yield increase in the U.S. Midwest. *Science* **2014**, *344*, 516–519. [CrossRef] [PubMed]
55. Tebaldi, C.; Lobell, D.B. Towards probabilistic projections of climate change impacts on global crop yields. *Geophys. Res. Lett.* **2008**, *35*, 2–7. [CrossRef]
56. Chen, H.; Xiong, L. Myo-Inositol-1-phosphate synthase is required for polar auxin transport and organ development. *J. Biol. Chem.* **2010**, *285*, 24238–24247. [CrossRef]
57. Landoni, M.; Badone, F.C.; Haman, N.; Schiraldi, A.; Fessas, D.; Cesari, V.; Toschi, I.; Cremona, R.; Delogu, C.; Villa, D.; et al. Low phytic acid 1 mutation in maize modifies density, starch properties, cations, and fiber contents in the seed. *J. Agric. Food Chem.* **2013**, *61*, 4622–4630. [CrossRef]
58. Wasson, A.P.; Richards, R.A.; Chatrath, R.; Misra, S.C.; Prasad, S.V.S.; Rebetzke, G.J.; Kirkegaard, J.A.; Christopher, J.; Watt, M. Traits and selection strategies to improve root systems and water uptake in water-limited wheat crops. *J. Exp. Bot.* **2012**, *63*, 3485–3498. [CrossRef]
59. Lynch, J.P.; Wojciechowski, T. Opportunities and challenges in the subsoil: Pathways to deeper rooted crops. *J. Exp. Bot.* **2015**, *66*, 2199–2210. [CrossRef]
60. Paez-Garcia, A.; Motes, C.M.; Scheible, W.R.; Chen, R.; Blancaflor, E.B.; Monteros, M.J. Root traits and phenotyping strategies for plant improvement. *Plants* **2015**, *4*, 334–355. [CrossRef]
61. Pilu, R.; Cassani, E.; Villa, D.; Curiale, S.; Panzeri, D.; Badone, F.C.; Landoni, M. Isolation and characterization of a new mutant allele of brachytic 2 maize gene. *Mol. Breed.* **2007**, *20*, 83–91. [CrossRef]
62. Avila, L.M.; Cerrudo, D.; Swanton, C.; Lukens, L. Brevis plant1, a putative inositol polyphosphate 5-phosphatase, is required for internode elongation in maize. *J. Exp. Bot.* **2016**, *67*, 1577–1588. [CrossRef]
63. Landoni, M.; Cassani, E.; Ghidoli, M.; Colombo, F.; Sangiorgio, S.; Papa, G.; Adani, F.; Pilu, R. Brachytic2 mutation is able to counteract the main pleiotropic effects of brown midrib3 mutant in maize. *Sci. Rep.* **2022**, *12*, 2446. [CrossRef] [PubMed]
64. Zhang, B.; Gao, Y.; Zhang, L.; Zhou, Y. The plant cell wall: Biosynthesis, construction, and functions. *J. Integr. Plant Biol.* **2021**, *63*, 251–272. [CrossRef] [PubMed]
65. Yeats, T.H.; Rose, J.K.C. The formation and function of plant cuticles. *Plant Physiol.* **2013**, *163*, 5–20. [CrossRef] [PubMed]